

N92-14910

Measurement of Laser Spot Quality

T.D. Milster, Optical Sciences Center, University of Arizona, Tucson, Arizona 85721  
 J.P. Treptau, Optical Sciences Center, University of Arizona, Tucson, Arizona 85721

Abstract

Several ways of measuring spot quality are compared. We examine in detail various figures of merit such as full-width-at-half maximum (FWHM), full-width-at-1/e<sup>2</sup> maximum, Strehl ratio, and encircled energy. Our application is optical data storage, but results can be applied to other areas like space communications and high-energy lasers. We found that the optimum figure of merit in many cases is Strehl ratio.

Introduction

There are several methods useful for measuring laser spot quality, such as interferometry, CCD cameras, and knife-edge scanners. Interferometric methods commonly use a lens to recollimate the light, as shown in Figure 1a. Measurements are highly precise with better than  $\lambda/100$  wavefront variation. However, there are certain difficulties involved in using an interferometer. The numerical aperture (NA) of the collecting optics must be greater than the NA of the beam. The collection optics may introduce aberrations into the beam. Also, it is tedious to align the interferometer. In some situations, the physical size of the interferometer is not convenient. CCD cameras avoid some of the alignment problems associated with interferometers. As shown in Figure 1b, a laser spot can be focused directly onto the CCD array. However, the sampling of the spot is limited by the pixel size, which is typically about  $10\mu\text{m}$  by  $10\mu\text{m}$ . Spot diameters of less than several hundred microns are difficult to measure accurately with a CCD. An auxiliary lens can be placed between the spot and the CCD, as shown in Figure 1c, but the NA of the collection optics must be greater than the NA of the beam. The alignment must also be done very carefully, and the optics must be carefully considered. For example, Bobroff et al. have constructed, with some difficulty, a very high quality system for measuring spots from lithographic lenses (1). A third option for measuring spot quality is to use a knife-edge scanner. The spot profile is estimated by scanning an opaque edge through the spot, as shown in Figure 1d. A detector records transmitted power versus time. The derivative of the knife-edge scan with respect to time,  $\delta i/\delta t$ , is the line scan of the spot, which is an estimate of the spot profile. The line scan is equivalent to scanning an infinitely thin slit, as shown in Figure 2. The slit integrates irradiance in the y direction. Therefore, the line scan is not exactly equivalent to the true spot profile. However, because of its small size

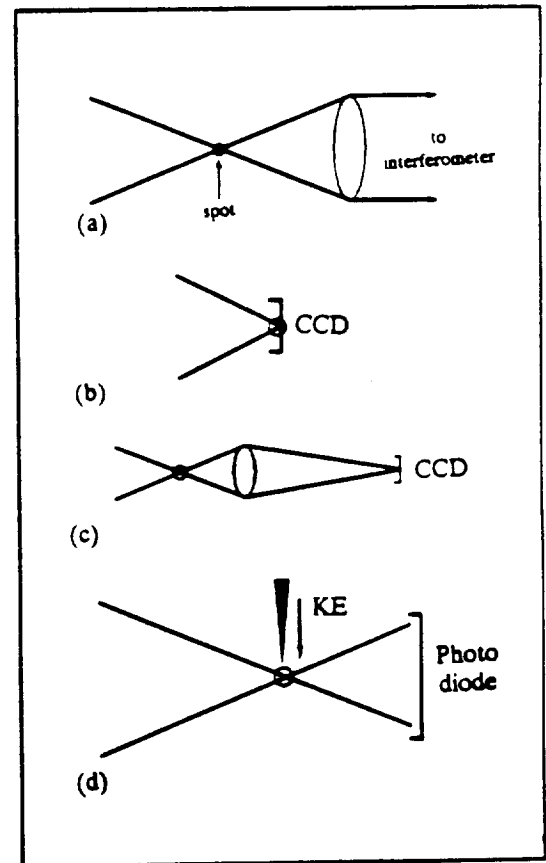


Figure 1. Measurement methods: (a) interferometric; (b) CCD direct; (c) CCD with aux. lens; (d) knife-edge scanner.

and direct output, the knife-edge technique is very convenient in the laboratory.

We can understand differences between the knife-edge scan and the true spot profile by analyzing the spot irradiance distribution in Figure 3a. Various amounts of aberration add to yield a wavefront standard deviation,  $\sigma$ , of  $\sigma = 0.077$ , which is just at the diffraction limit. The spot is slightly elongated in a diagonal direction, which is most easily observed in the 5% irradiance contour level. The true spot profile and the knife-edge scan ( $\delta i / \delta t$ ) are shown in Figure 3b. Since the knife-edge scan integrates the spot distribution in one direction, it indicates a wider profile than the true spot.

Each measurement method can produce various figures of merit for the spot. The standard deviation of the wavefront,  $\sigma$ , can be found from interferometric data. The full-width-at-half maximum (FWHM) is shown in Figure 4a. The full-width-at- $1/e^2$  maximum (FW $1/e^2$ ) is shown in Figure 4b. The Strehl ratio is defined as the ratio of the maximum irradiance of the aberrated spot to the maximum irradiance of an unaberrated spot, as shown in Figure 4c. Encircled energy is defined as the ratio of the power delivered in a circular area surrounding the maximum of the aberrated spot to power in the same area around the maximum of the unaberrated spot, as shown in Figure 4d.

Our application is measuring sub-micron spot profiles for optical data storage devices. The NA is typically between 0.45 and 0.60. Wavelengths are in the range of 780nm to 830nm. Spot sizes are typically too small for direct CCD measurements. Interferometric methods are commonly used

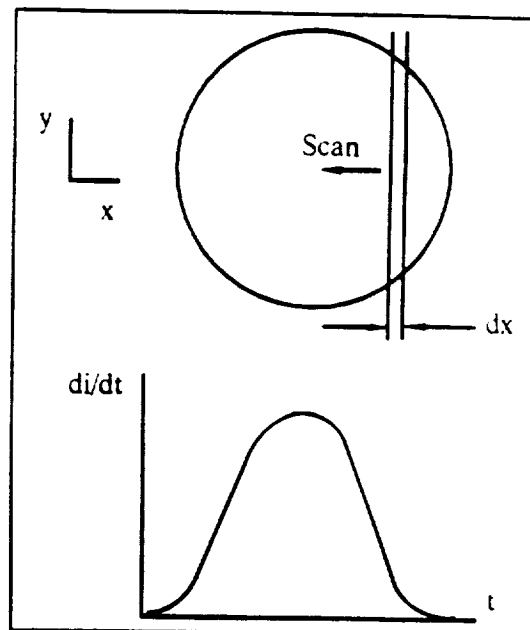


Figure 2. The derivative of the knife-edge scan is equivalent to scanning an infinitely thin slit across the spot. (a) slit scan; (b)  $\delta i / \delta t$ .

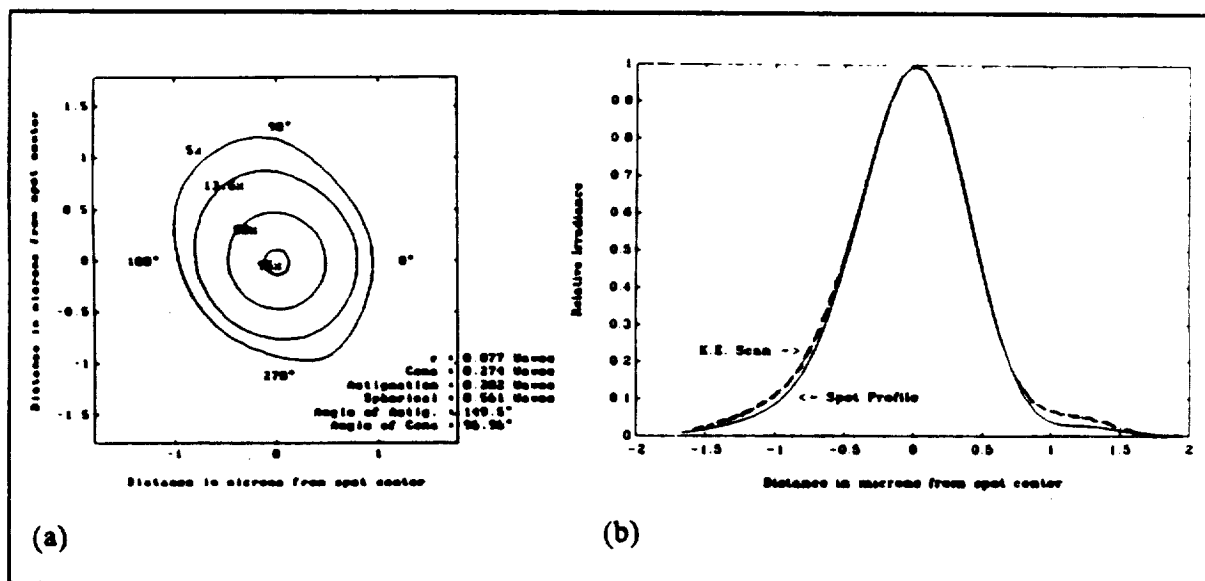


Figure 3. (a) An aberrated spot that shows an asymmetric irradiance profile is analyzed. The value  $\sigma = 0.077$  is near the diffraction limit; (b) Differences between the knife-edge scan through the spot and the true spot profile are shown.

to test collimated light beams in the optical path, but they are not used for testing the focussed spot. Instead, some form of knife-edge scanner is used. Modified CCD devices are of questionable utility due to the large NA. Size and quality of the focused spot is very important because small spots yield high data densities. Historically, FWHM has been used as a metric for spot quality.

Other applications use similar figures of merit. In high-energy laser work and space-laser communications, the full width of the far-field divergence angle is typically used. The motivation is to deliver as much energy as possible to the receiver. However, it is often the case that a substantial amount of energy falls outside of the central peak.

This paper addresses differences between various figures of merit for measuring beams with small amounts of aberration. We consider only spherical, coma, and astigmatic aberrations. We restrict our attention to beams that are near or under Marechal's criterion for diffraction-limited performance (2), that is  $\sigma \leq 1/14$  waves. For larger amounts of aberration, some figures of merit become difficult to interpret. For example, it would be very difficult to determine FWHM for Figure 5, which illustrates a spot aberrated with 0.8 wave of coma, 0.8 wave of astigmatism, and 1.6 waves of spherical. Piston, tilt, and defocus have been added to minimize wavefront variance. This brings the spot into best possible focus. Our results are based on a computer simulation.

### Simulation

We analyze an optical data storage system that focuses light from a laser diode to a disk medium. An illustration of the optical path is shown in Figure 6. The laser diode has different divergence angles in the parallel and perpendicular directions with respect to the junction. Circularization optics are used after a collimator to make the beam more uniform. A partially-polarizing beam splitter is used to direct the reflected light from the disk to data and servo detectors. The stop is located at the objective lens, which focuses light on the disk. Our system parameters include  $NA = 0.55$ ,  $f_o = 4.0$  mm, and  $\lambda = 780$  nm. The amplitude distribution in the pupil is Lorentzian in the direction perpendicular to the junction and Gaussian in the direction parallel to the junction. The widths of the amplitude distribution were adjusted for the best tradeoff between power throughput and spot size (3). The unaberrated FWHM is approximately  $0.9\mu\text{m}$  in the direction perpendicular to the junction and  $0.87\mu\text{m}$  in the direction parallel to the junction. Random amounts of aberration were added to the pupil for each trial, and the proper amount of piston, tilt, and defocus were added in order to bring the spot into best focus. Standard deviation

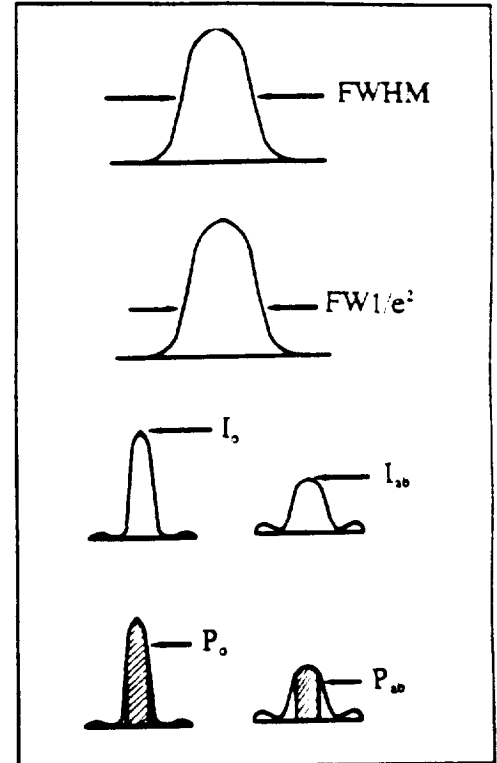


Figure 4. Various figures of merit. (a) FWHM; (b)  $FW1/e^2$ ; (c) Strehl ratio =  $I_{ab}/I_o$ ; (d) encircled energy =  $P_{ab}/P_o$ .

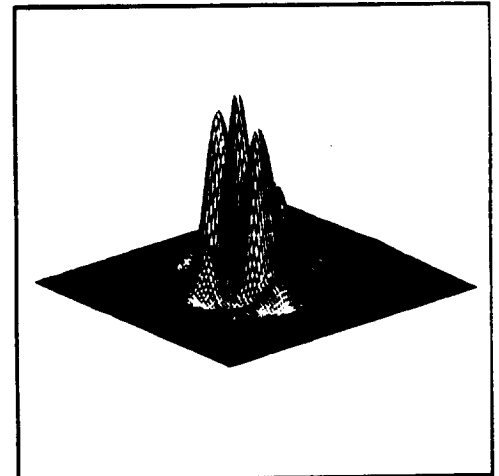


Figure 5. 0.8 wave coma, 0.8 wave astigmatism, and 1.6 waves spherical at best focus.

of the wavefront was kept between the limits:  $0 \leq \sigma \leq 0.10$ . Random parameters included spherical, coma, coma rotation angle, astigmatism, and astigmatism rotation angle. The diffracted spot was calculated with scalar diffraction theory. Figures of merit were calculated for each trial, and the results are plotted versus standard deviation of the wavefront. We calculate figures of merit for both the true spot profile and the knife-edge scan.

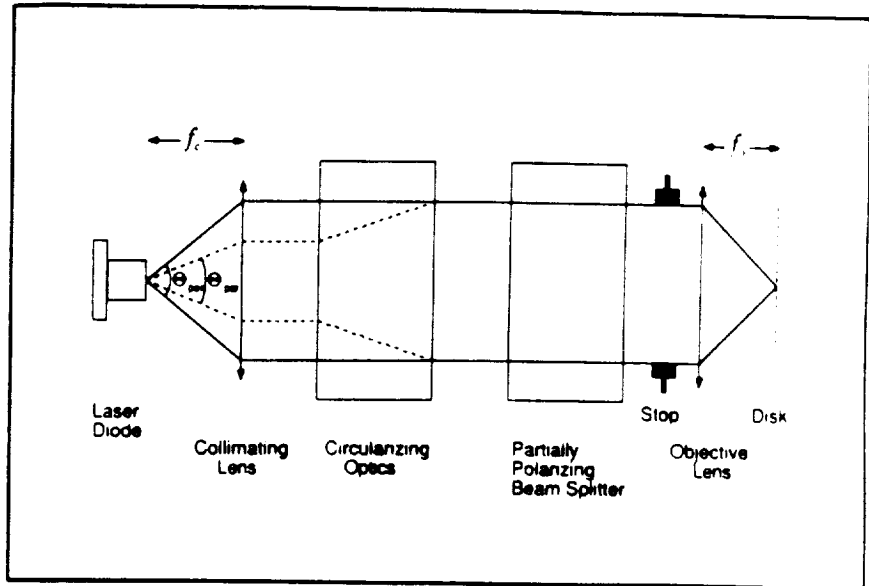


Figure 6. MO storage device (laser to disk).

### Results

Figure 7 displays results for FWHM. For low values of  $\sigma$ , the FWHM in  $x$  and  $y$  directions (perpendicular and parallel to the junction, respectively) are not equal. This is due to Gaussian/Lorentzian filling of the aperture. Also, the knife-edge scan is not equivalent to the true spot profile. This is because of the line-scan integration. As  $\sigma$  is increased, FWHM does not increase noticeably. Near the diffraction limit,  $\sigma \approx 0.07$ , FWHM starts fluctuating significantly, which indicates a poor correlation between FWHM and  $\sigma$ . As  $\sigma$  is increased beyond the diffraction limit, the four different measures are very dependent on the amount and rotation angle of the aberration.

The fact that width measurements are not very sensitive to small amounts of aberration may be understood by examining the difference between aberrated and unaberrated spots. Figure 8 displays an aberrated spot with 0.955 waves of spherical and the appropriate amount of defocus. The difference is also displayed, which shows that energy is taken from the central lobe and placed in the outer rings. The difference function passes through zero at the first dark ring. Therefore, the width of the central lobe is constrained. Any changes

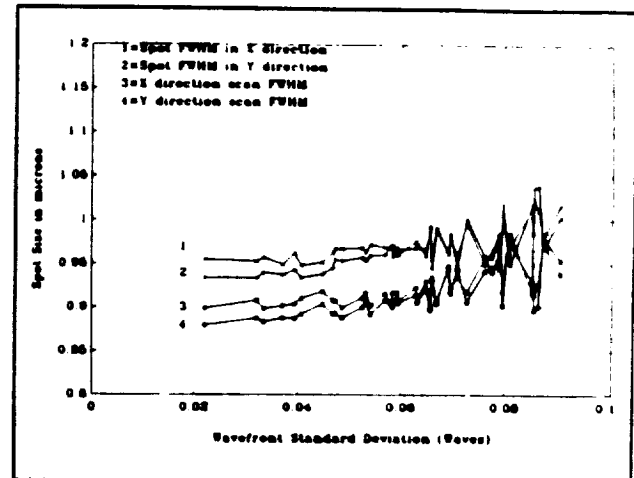


Figure 7. FWHM from the computed spot and knife-edge scans.

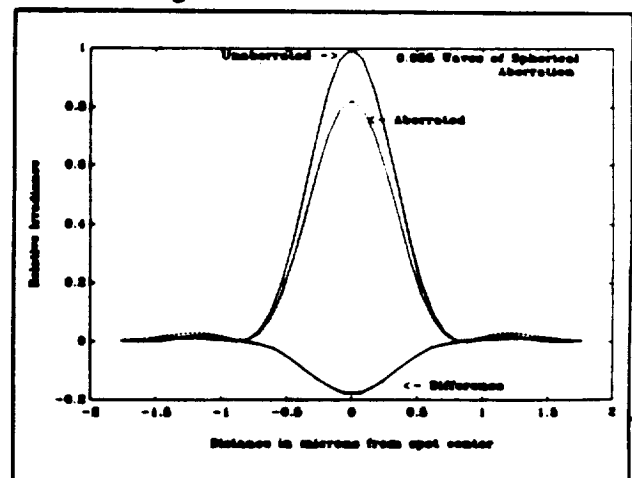


Figure 8. Aberration contribution to the spot profile with 0.955 wave of spherical and the appropriate amount of defocus.

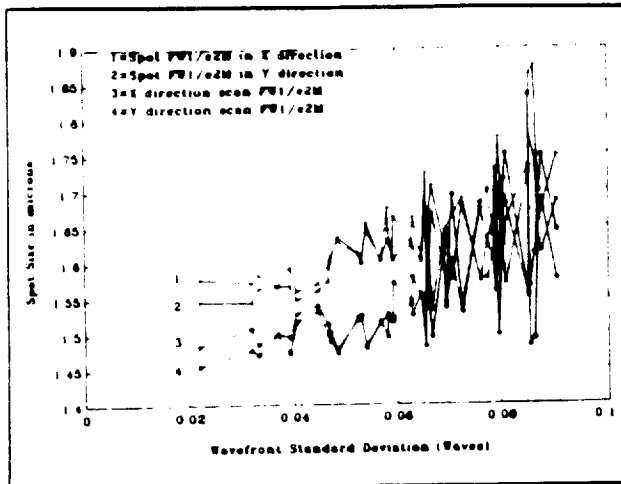


Figure 9. FW1/e<sup>2</sup> from the computed spot and knife-edge scans.

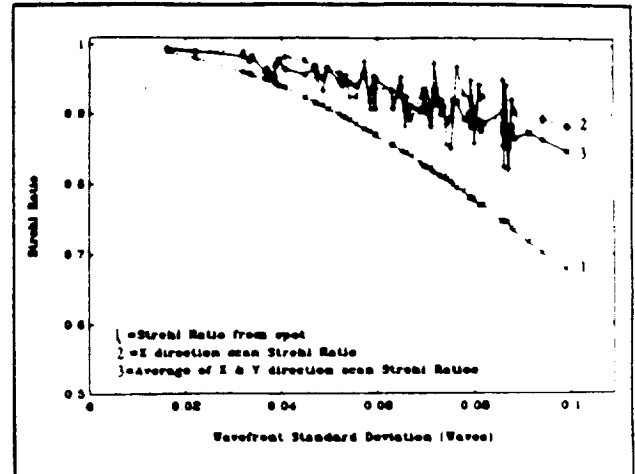


Figure 10. Comparison of Strehl ratio from computed spot and knife-edge scans.

in width of the central lobe are secondary effects. Similar results are obtained with other aberrations.

Figure 9 displays results for FW1/e<sup>2</sup>. Differences between spot and knife-edge scan are observed at low values of  $\sigma$ , which are due to integration of the line scan. Differences also are observed between x and y profiles, which are due to Gaussian/Lorentzian filling of the aperture. As  $\sigma$  increases, FW1/e<sup>2</sup> generally increases, but it quickly becomes poorly correlated with  $\sigma$ . The FW1/e<sup>2</sup> is very sensitive to the kinds of aberrations present and their orientations.

Figure 10 displays results for Strehl ratio. The Strehl ratio for the spot followed Marechal's relationship (2), that is,  $SR = 1 - (2\pi/\lambda)^2 \sigma^2$ . Fluctuations in Strehl ratio for the spot measurement are very small. Strehl ratio for the knife-edge scan in the x direction fluctuates considerably. Strehl ratio for the knife-edge scan in the y direction (not shown) also fluctuates considerably. A smoother curve is generated by taking the average of x and y scans. The average decreases with increasing  $\sigma$ , which indicates a reasonable figure of merit.

Figure 11 displays results for encircled energy. As with the Strehl ratio results, a comparatively smooth curve is generated by taking an average of the x and y scans. The averages for 2 $\mu$ m, 1 $\mu$ m and 0.5 $\mu$ m effective widths from the knife-edge scans are shown. The encircled energy for a 0.25 micron diameter pinhole over the spot is also shown. The noise-like variations in encircled energy versus  $\sigma$  are approximately equivalent for the data shown. The average of the 0.25 $\mu$ m

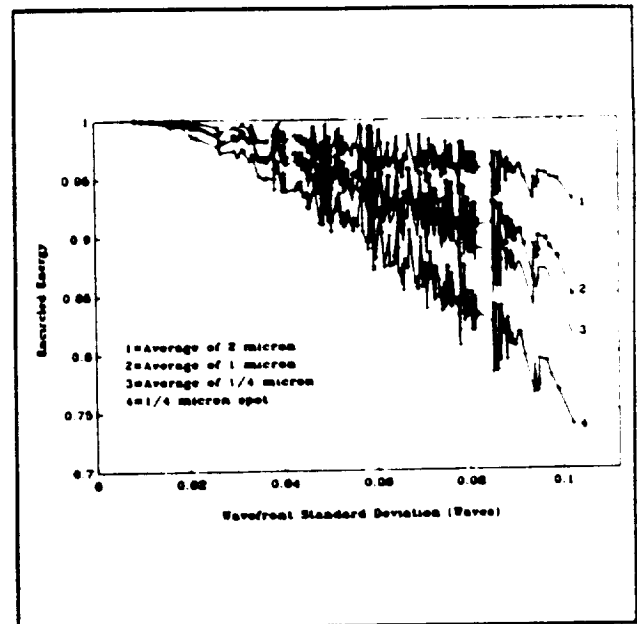


Figure 11. Encircled energy: average of scans and 0.25 $\mu$ m diameter spot pinhole.

knife-edge scan is comparable to the average Strehl-ratio data of Figure 10. This suggests that an adequate integration range around the central peak is about  $100\% \times 0.25/0.9 = 28\%$  of the unaberrated spot FWHM.

### Conclusions

We have illustrated several important points about measurement of laser spot quality. First, results from knife-edge scans and actual spot profiles differ due to the integration of the differentiated knife-edge signal. Secondly, width measurements are not adequate (by themselves) to describe spot quality. This is because width of the central lobe is constrained by pupil filling for small amounts of aberration, and, for large amounts of aberration, width measurements are difficult to interpret. Thirdly, the most sensitive measure of spot quality for many applications is the Strehl ratio. The Strehl ratio is difficult to measure directly, but it may be approximated by averaging the encircled energy found from  $x$  and  $y$  scans of a knife-edge scanner. The integration range should be no more than about 28% of the unaberrated spot FWHM.

### References

1. N. Bobroff, P. Fadi, A.E. Rosenbluth, and D.S. Goodman, "Bench evaluation of lithographic lenses from measurements of the point spread function," *Proc SPIE* 922, pp. 376-386, 1988.
2. M. Born and E. Wolf, Principles of Optics, 6th ed., Pergammon Press, New York, p 469 (1986).
3. H.M. Haskal, "Laser recording with truncated Gaussian beams," *Appl. Opt.*, vol. 18 no 13, pp. 2143-2146 (1979).